Letter

Fluctuation-induced interactions and the spin-glass transition in Fe_2TiO_5

P. G. LaBarre,[1] D. Phelan,[2] Y. Xin,[3] F. Ye,[4] T. Besara,[3,5] T. Siegrist,[3,5] S. V. Syzranov,[1] S. Rosenkranz,[2] and A. P. Ramirez[1]

[1]*Physics Department, University of California Santa Cruz, Santa Cruz, California 95064, USA*

[2]*Materials Science Division, Argonne National Laboratory, Lemont, Illinois 60439, USA*

[3]*NHMFL, Florida State University, Tallahassee, Florida 32310, USA*

[4]*Neutron Scattering Division, Oak Ridge National Laboratory, Oak Ridge, Tennessee 37830, USA*

[5]*Department of Chemical and Biomedical Engineering, FAMU-FSU College of Engineering, Tallahassee, Florida 32310, USA*

(Received 29 May 2019; revised 4 November 2020; accepted 24 May 2021; published 11 June 2021; corrected 22 June 2021 and 20 July 2021)

We investigate the spin-glass transition in the strongly frustrated well-known compound Fe_2TiO_5. A remarkable feature of this transition, widely discussed in the literature, is its anisotropic properties: The transition manifests itself in the magnetic susceptibly only along one axis, despite Fe^{3+} d^5 spins having no orbital component. We demonstrate, using neutron scattering, that below the transition temperature $T_g = 55$ K, Fe_2TiO_5 develops nanoscale surfboard-shaped antiferromagnetic regions in which the Fe^{3+} spins are aligned perpendicular to the axis which exhibits freezing. We show that the glass transition may result from the freezing of transverse fluctuations of the magnetization of these regions and we develop a mean-field replica theory of such a transition, revealing a type of *magnetic* van der Waals effect.

DOI: 10.1103/PhysRevB.103.L220404

Magnetic materials play a central role in condensed-matter physics due to the breadth of fundamental phenomena resulting from the spin degrees of freedom and their mutual interactions [1,2]. This allows many-body theories, in which the spin's size, dimensionality, anisotropy, and interaction range are variables, to accurately describe the properties of a wide range of different systems [3]. Of interest here is spin glass (SG), a collective state displaying a cusp in the temperature-dependent susceptibility [$\chi(T)$] but lacking long-range order [4]. As Anderson noted [5], SG arises from the combined effects of frustration of the antiferromagnetic (AF) interactions and quenched atomic disorder. The interplay of these factors results in a landscape of metastable states into which the spins fall and cease fluctuating in time, or freeze, below a critical "glass" temperature, T_g. Since the degrees of freedom are atomic spins with conserved magnitude, a signature of freezing in one direction is connected to a similar response in the other directions, a connection manifested even at the mean-field level.

It is an enduring puzzle, therefore, that Fe_2TiO_5, in which all of the Fe^{3+} spins are purely s state and thus isotropic, exhibits a cusp in $\chi(T)$ *only in one direction*, as shown in Fig. 1. This feature of Fe_2TiO_5 has puzzled physicists over several decades and has triggered a flurry of research [6–12] including a neutron-scattering study that confirmed the lack of long-range order below $T_g = 55$ K [6]. While one theory introduces anisotropy in a phenomenological way [8], the microscopic source of anisotropy, at the heart of the puzzle, has not been addressed. Here we present linear $\chi(T)$, nonlinear susceptibility $\chi_3(T)$, and neutron-scattering data that show, on cooling towards T_g, the growth of nanoscale surfboard-shaped regions of AF-ordered spins aligned along an axis transverse to the freezing direction. We argue, using the replica formalism, that SG freezing is induced by fluctuations in the transverse magnetization between surfboard spins, an experimental observation of a magnetic analog to the van der Waals force.

For the present study we used single crystals of Fe_2TiO_5 grown by Remeika [13]. The pseudobrookite structure of A_2BO_5 with space group *Cmcm* was confirmed by x-ray diffraction. We note that the Fe^{3+} and Ti^{4+} ions share the A and B sites: the A site contains 0.64 Fe and 0.36 Ti while the B site contains 0.72 Fe and 0.28 Ti. To confirm that all the Fe ions are in the isotropic Fe^{3+} state, electron energy-loss spectroscopy (EELS; see Supplemental Material [14]) was used. We find both $L3$ and $L2$ spectra that are fully consistent with only Fe^{3+}. Thus, the concentration of magnetic ions (Fe^{3+}) can be taken as 2/3 on both A and B sites with random site occupation.

Magnetization measurements were performed in two different magnetic property measurement systems. For $\chi(T)$ and $\chi_{nl}(T)$ for $T < 300$ K, a conventional sample holder was used. For measurements with 300 K $< T <$ 900 K, the sample was mounted with Zircar cement on a rod designed for high-temperature studies. The leading nonlinear susceptibility ([(T)]) was obtained by measuring magnetization (M) as a function of magnetic field ($\boldsymbol{H}$) at fixed T. The $M(\boldsymbol{H})$ data were fit to a sum of polynomials ($\chi_0 + \chi_1 H + \chi_3 H^3$). Neutron-scattering measurements were performed on the *Corelli* instrument [15] at the Spallation Neutron Source at Oak Ridge National Laboratory from 5–300 K. *Corelli* employs a broad band of incident neutron energies to perform time-of-flight Laue diffraction measurements and simultaneously provides both the energy integrated signal, e.g., the equal-time two-particle correlation function, as well as the purely elastic signal, through implementing cross correlation

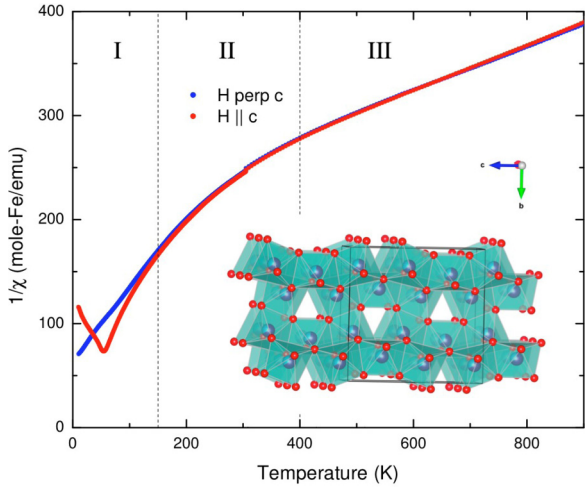

FIG. 1. Inverse susceptibility of Fe_2TiO_5 for H perpendicular and parallel to the c axis. Inset: structure of Fe_2TiO_5 showing the Fe/Ti sites (blue balls) and oxygen (red balls).

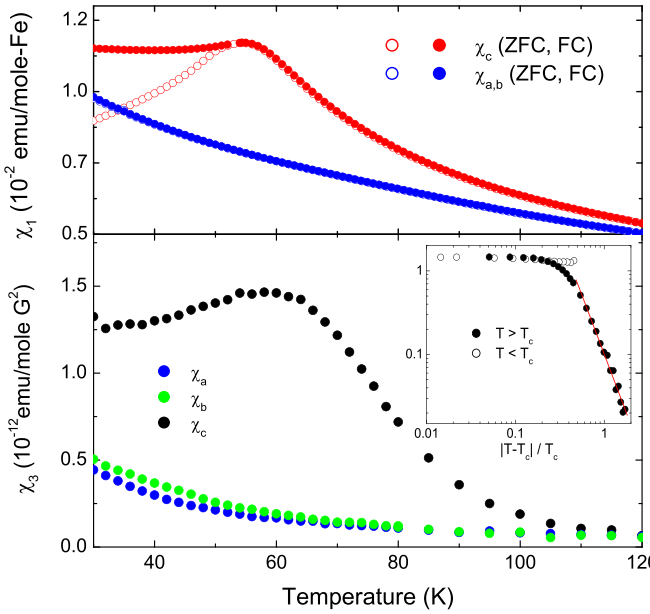

FIG. 2. Top: Linear susceptibility (χ_1) in the c and a, b directions, for cooling in zero field (ZFC) and cooling in a field (FC) of $H = 0.1$ T. Bottom: Nonlinear susceptibility (χ_3) for the a, b, and c directions showing a peak at the freezing temperature, T_g, in the c direction. The inset shows the power-law behavior critical behavior above T_g and the straight line corresponds to $\gamma = 2.72$, as discussed in the text.

with a pseudorandom chopper [16]. Measured raw neutron data were transformed and put into uniform sized bins in momentum transfer space (h, k, l) using the MANTID software package [17,18].

The inverse susceptibility from 5 to 900 K is shown in Fig. 1. We find an effective moment ($\mu_{\rm eff}$) for $\boldsymbol{H}||\boldsymbol{c}$ and $\boldsymbol{H}\perp\boldsymbol{c}$ to be 6.07 and 6.18 μ_B, respectively, in reasonable agreement with an s-state moment of $S = 5/2$ ($\mu_{\rm eff} = 5.92\,\mu_B$) and a g factor of 2.06. The antiferromagnetic (AF) Weiss constant (θ_W) is found to be 893 and 948 K for $\boldsymbol{H}||\boldsymbol{c}$ and $\boldsymbol{H}\perp\boldsymbol{c}$, respectively. Since the Fe^{3+} occupation is 2/3 of all A and B sites, these θ_W values represent 2/3 that of the structure fully occupied with Fe^{3+}, which is not attainable. In Fig. 2 are shown $\chi_1(T)$ and $\chi_3(T)$. The behavior of $\chi_1(T)$ is similar to that previously reported [6], exhibiting SG freezing below T_g K for $\boldsymbol{H}||\boldsymbol{c}$, with no anomaly in the other two directions. This conclusion is supported by measurements of $\chi_3(T)$ for $\boldsymbol{H} \parallel \boldsymbol{c}$ where a peak is seen at T_g. While there is only a weak decrease in $\chi_3(T)$ below T_g, the high-temperature behavior obeys the form $\chi_3(T) = t^{-\gamma}$, Fig. 2 (inset), where $t = |T - T_g|/T_g$ and the critical exponent $\gamma = 2.72 \pm 0.09$. This value of γ is larger than for canonical SGs, which exhibit $\gamma \approx 2.1-2.3$ [4], a result that is consistent with the neutron-determined correlation lengths discussed below. It is not unusual for SGs to develop Ising character, but the situation in Fe_2TiO_5 is qualitatively different since the response for $\boldsymbol{H}\perp\boldsymbol{c}$ is completely independent of the singularity observed for $\boldsymbol{H} \parallel \boldsymbol{c}$. As alluded to above, this behavior is incompatible with a mean-field description of a SG based on atomic spins, and suggests that the degree of freedom itself emerges from a collective effect.

To probe collective effects amongst the atomic spins, we performed neutron-scattering measurements. The upper panels of Figs. 3(a) and 3(b) show the elastic neutron-scattering intensity measured at $T = 5$ K in the ($hk0$) and ($^1/_2kl$) planes, respectively. Here, we utilize relative reciprocal lattice units for the wave-vector transfer $\mathbf{Q} = (h \times 2\pi/a,\ k \times 2\pi/b,\ l \times 2\pi/c)$, with orthorhombic lattice constants $a = 3.732$ Å, $b = 9.8125$ Å, and $c = 10.0744$ Å. Streaks of scattering along $\boldsymbol{b}^*$ are seen both in the ($hk0$) plane at half-integer values of h, as well as in the ($^1/_2kl$) plane at integer values of l. The presence of these streaks, well within the SG state, indicates that the correlation length (ζ_b) along $\boldsymbol{b}$ remains short, limited to one or two nearest neighbors, while ζ_a and ζ_c both have grown to at least an order of magnitude larger than ζ_b. While the pseudobrookite structure gives rise to a rather complex spin lattice, nearest spins are simply separated by a lattice unit a along $\boldsymbol{a}$. The occurrence of narrow peaks along $\boldsymbol{a}^*$ at half-integer values of h therefore immediately reveals the presence of strong AF correlations between neighboring spins along $\boldsymbol{a}$. Furthermore, cuts through these diffuse streaks of scattering along $\boldsymbol{a}^*$ or $\boldsymbol{c}^*$ are well represented by resolution-broadened Lorentzian line shapes, from which we extract correlation lengths of $\zeta_a = 42$ Å and $\zeta_c = 12$ Å at $T = 5$ K. Cuts along $\boldsymbol{b}^*$ [see Fig. 3(c)] however are very broad, do not peak at integer or half-integer reciprocal lattice positions, and are poorly represented by Lorentzian profiles. This clearly indicates that the correlations are limited to a few nearest spins only along $\boldsymbol{b}$.

These observations allow us to develop a model of the spin arrangement as follows. First, we assume that both A and B sites are fully occupied by Fe^{3+} spins. We find that the $\boldsymbol{b}^*$ dependence is well reproduced when correlations along $\boldsymbol{b}$ are limited to nearest neighbors within the same $\boldsymbol{a}$-$\boldsymbol{c}$ plane in the form of corrugated double chains, as indicated in Fig. 4(a). Including correlations that extend further along $\boldsymbol{b}$ to spins between different $\boldsymbol{a}$-$\boldsymbol{c}$ planes, e.g., spins in the $y = 0$ and $y = {}^1/_2$ planes, immediately leads to much sharper peaks than observed, showing that the development of spin correlations along $\boldsymbol{b}$ is strongly suppressed. A likely scenario is

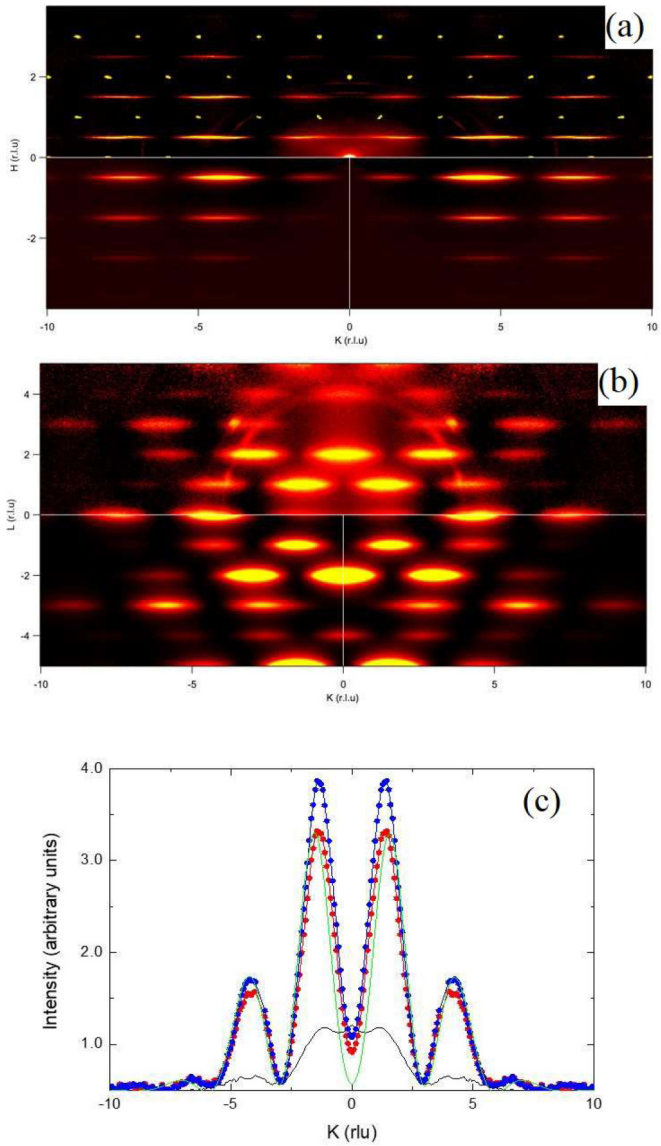

FIG. 3. Elastic neutron-scattering intensity in the (a) [h, k,0] and (b) [0.5, k, l] planes at $T = 5$ K. The upper panels show the measured intensities with Bragg peaks visible in (a). The lower left panels show the intensities for the simulations as described in the text for the structure with both A and B sites fully occupied by Fe^{3+} spins (left panels) and for a random occupation of 1/3 of the positions with $s = 0$ (lower right panels), (c) Neutron-scattering intensity along the k direction for $Q = (0.5, k, 1)$ showing the purely elastic (red dots) as well as total scattering (blue squares) at $T = 6$ K and the much weaker total scattering at 300 K. The green solid line is the calculated intensity as described in the text.

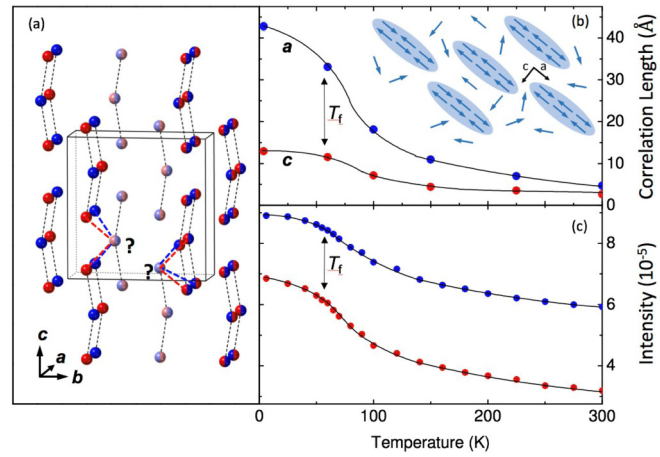

FIG. 4. (a) Illustration of the low-temperature spin order in Fe_2TiO_5. Only the Fe/Ti positions are shown, assuming that all positions are fully occupied with Fe spins with blue (red) spheres denoting the up (down) positions along the a direction. The spheres at right are half colored, denoting the lack of Long Range Order. The spins are AF aligned within the triplets indicated with light dashed lines, forming corrugated double chains (in planes at integer x positions). Along the b direction, the next such double chain is centered at half-integer x positions, and since the spins are AF aligned along the a axis, each spin at the half-integer positions sees a net zero mean field. (b) Correlation lengths in the a and c directions vs temperature. (c) Temperature dependence of total (blue) and elastic (red) neutron-scattering intensity over the wave-vector range $Q = (0.5 \pm 0.1, 4.25 \pm 0.95, 0 \pm 0.1)$.

the complete suppression of the exchange fields from spins in the $y = 0$ and $y = 1$ planes seen by a spin in the $y = 0.5$ plane due to AF alignment along $\boldsymbol{a}$ and the centering of the *Cmcm* space group [see Fig. 4(a)]. The direction of spin alignment can be inferred by observing that in the (hk0) plane [Fig. 3(a)], the neutron-scattering intensity vanishes along $\boldsymbol{a}^*$, e.g., for wave vectors $\mathbf{Q} = (h,0,0)$. This indicates that the spins point parallel or antiparallel to $\boldsymbol{a}$, since only the spin component perpendicular to the wave vector contributes to the magnetic neutron-scattering cross section [19]. In contrast, if the spins were pointing along $\boldsymbol{b}$, the intensity would be maximized along $\mathbf{Q} = (h,0,0)$ but strongly suppressed at $\mathbf{Q} = (0.5,k,0)$, which is clearly not the case [see Figs. 3(a) and 3(b), respectively]. Based on this model, we calculate the neutron-scattering intensity according to

$$\frac{\partial\sigma}{\partial\Omega} \sim \sum_{\alpha,\beta}\left(\delta_{\alpha\beta} - \hat{Q}_\alpha\hat{Q}_\beta\right) f(Q)^2 \sum_{\substack{i,\,j \\ i\neq j}} \langle S_i \cdot S_j\rangle \, e^{-iQ\cdot(R_j - R_i)}, \tag{1}$$

where $f(\boldsymbol{Q})$ is the magnetic form factor for Fe^{3+}, $\alpha, \beta = x, y, z$, and S_i the spin at position R_j. Here, we approximate the decay of the spin correlations along $\boldsymbol{a}$ and $\boldsymbol{c}$ in the Ornstein-Zernike form utilizing the correlation lengths ζ_a and ζ_c obtained from the Lorentzian fits to the data [20]:

$$\langle \boldsymbol{S}_i \cdot \boldsymbol{S}_j\rangle = \boldsymbol{S}_i \cdot \boldsymbol{S}_j \, \frac{e^{-\left(\frac{|x_j - x_i|}{\zeta_a} + \frac{|z_j - z_i|}{\zeta_c}\right)}}{|\boldsymbol{R}_j - \boldsymbol{R}_i|}. \tag{2}$$

The simulated neutron intensity is then obtained by summing Eq. (1) over a box that is much larger than ζ_a and ζ_c along $\boldsymbol{a}$ and $\boldsymbol{c}$, respectively, but very narrow along $\boldsymbol{b}$, spanning only half a unit cell (e.g., only one double chain along $\boldsymbol{b}$) as required in order to reproduce the k dependence of the observed neutron-scattering intensity. The simulated neutron intensity so obtained is in overall good qualitative agreement with the observation [see lower panels of Fig. 3(a) and Fig 3(b)]. We

then repeat the calculation with a random distribution of 33% of each site with spin $\boldsymbol{S}_i = 0$, close to the distribution of (Fe,Ti) in Fe_2TiO_5. The resulting simulated intensity [lower right panels of Fig. 3(a) and Fig. 3(b)] is again in good qualitative agreement with the observation, and qualitatively not different from the results in which all sites are fully occupied with Fe^{3+} spins.

Figure 4(c) shows the temperature dependence of both the *elastic* and the energy-integrated (total) scattering intensity integrated over one of the broad peaks along k at $\boldsymbol{Q} = (0.5, 3.3–5.2, 0)$. At high temperature, the total scattering is much stronger than the elastic signal, reflecting the presence of fluctuating spin correlations and an elastic signal only present because of the quasielastic nature of the fluctuations. Upon cooling, the elastic signal increases faster than the total signal, with a marked sharp increase below 100 K and an inflection point near T_g, signaling the onset of spin freezing. However, the elastic signal remains weaker than the total signal down to 5 K, indicating that spin fluctuations are still present at base temperature. The correlation lengths along $\boldsymbol{a}$ and $\boldsymbol{c}$ further show the rapid growth of spin correlations along $\boldsymbol{a}$ upon cooling whereas along $\boldsymbol{c}$, substantial correlations only become apparent below 150 K; see Fig 4(b).

The neutron measurements describe a situation shown schematically in Fig. 4(b), namely a low-temperature state of elongated, surfboard-shaped correlated regions in which the spins are aligned (anti)parallel to $\boldsymbol{a}$. While the fraction of Fe^{3+} spins occupying these regions is not known, the continuing increase of $\chi(T)$ along $\boldsymbol{a}$ and $\boldsymbol{b}$ on cooling below T_g suggests that a sizable fraction of spins are located in between surfboards, a region we will refer to as the *cloud*. Assuming that all of the anisotropy in spin space is associated with surfboard formation, a natural source of such anisotropy is the spin orientation in the surfboards. As is well known, $\chi(T)$ of a Heisenberg antiferromagnet becomes anisotropic below the Néel temperature T_N—along the ordered-spin direction, $\chi(T)$ approaches zero as $T \to 0$, whereas transverse to this direction, $\chi(T)$ remains finite. Absent crystal-field anisotropy, the spin direction is fixed to the crystal structure by the dipole-dipole energy, usually very small—e.g., in MnF_2 this energy is only a few K whereas $T_N = 67$ K [21]. Here, the intrasurfboard spins order with an AF pattern in registry with the lattice, along $\boldsymbol{a}$**,** but should retain a near-constant susceptibility transverse to $\boldsymbol{a}$, suggesting a scenario in which the $\boldsymbol{c}$-direction fluctuations in magnetization induce an interaction with other surfboards—a type of *magnetic* van der Waals interaction.

In order to assess the feasibility that such a van der Waals-type interaction can lead to SG freezing, we consider a model of the surfboard free energy, given by

$$F(\boldsymbol{M}) = \sum_i g(M_i) - \frac{1}{2}\sum_{i,j} J_{ij} M_i M_j. \tag{3}$$

where the indices i and j label the surfboards, $g(M)$ is a large positive definite function with a minimum at $M = 0$; the interaction $J_{ij} = J(\boldsymbol{r}_i - \boldsymbol{r}_j)$ between the surfboards at random positions $\boldsymbol{r}$ is weak and vanishes when averaging over the direction of the vector $\boldsymbol{r}_i - \boldsymbol{r}_j$, which is obeyed, for example, by dipole-dipole interactions [14].

To study the glass transition, we consider the disorder-averaged partition function of the system in the replica representation [22] in the form

$$Z = \int \mathcal{D}M \exp\left(-\frac{1}{T}\left[\sum_{i,\alpha} g\left(M_i^\alpha\right) - \frac{1}{4VT}\sum_{i,j\neq i,\alpha,\gamma} J_2 M_i^\alpha M_i^\gamma M_j^\alpha M_j^\gamma\right]\right), \tag{4}$$

where α and γ is the replica index and n and $J_2 = \int J(\boldsymbol{r})^2 d\boldsymbol{r}$. The replicated partition function (4) may be derived from the free energy (3) in the mean-field approximation, i.e., assuming that products of magnetizations fluctuate weakly on top of their average values. Going beyond the mean-field approximation will only shift the phase boundary of the glass phase by a factor of order unity.

We develop a mean-field theory of the transition [14] with the glass order parameter [22,23] $\mathbb{Q}^{\alpha\gamma} = \frac{1}{V}\sum_i M_i^\alpha M_i^\gamma$. In the replica-symmetric approximation ($\mathbb{Q}^{\alpha\gamma} = q$ for all $\alpha \neq \gamma$), the free energy of the system of surfboards is given by

$$F(q) = q^2 \frac{V J_2(T)}{4T}\left[\frac{J_2(T) n_0(T)}{T^2}\langle M^2\rangle^2 - 1\right] + O(q^4), \tag{5}$$

where $\langle M^2\rangle$ is the average square of the fluctuation of the magnetization M of one surfboard and n_0 is the spatial density of the surfboard. The free energy (5) signals a phase transition at $(J_2 n_0/T^2)\langle M^2\rangle^2 = 1$.

We can write $\chi(T) = n_0\langle M^2\rangle/T$, and the condition for the transition becomes $1 = (\chi^2/n_0)\int J(\boldsymbol{r})^2 d\boldsymbol{r}$. If we assume also that the interactions between the surfboards are dipole-dipole interactions [$J(r) \sim 1/(\mu r^3)$], the transition occurs at

$$\mu^2 n_0 r_0^3 \sim \chi^2, \tag{6}$$

where r_0 is the average cluster size and μ is the magnetic permeability. We consider χ in Eq. (6) to be the difference between $\boldsymbol{H} \parallel \boldsymbol{c}$ and $\boldsymbol{H} \perp \boldsymbol{c}$ at T_g, namely the surfboard contribution to the susceptibility, which yields a value of 1.7×10^{-4} in dimensionless units. Thus, for $\mu = 1$, appropriate for a cloud spin medium with a similarly small susceptibility, this implies that the ratio of the average surfboard size to the average separation between surfboards is $n_0^{1/3} r_0 = 7.0 \times 10^{-3} = 1/320$. This estimated value of $n_0^{1/3} r_0$ implies an extremely long-range interaction among surfboards but such a large disparity between the size and separation of surfboards is likely a result of the mean-field approximation used to derive Eq. (6). Specifically, in 3D it is known that mean-field treatments can overestimate the freezing temperature by more than a factor of 2 [24,25]. In addition, the absence of correlation length growth along $\boldsymbol{b}$ suggests that the effective dimensionality of our system is between 3D and 2D, the latter of which is

thought to exhibit a SG transition only at $T = 0$. Thus, a more exact confrontation of our model with experimental data will likely come from computational studies. While higher Fe density is not possible without compromising charge neutrality, compounds with lower Fe density will be studied in order to further test the theoretical prediction in Eq. (6).

In conclusion, we have shown that the anomalous spin-glass freezing in Fe_2TiO_5 is associated with the growth of nanoscale surfboard-shaped regions of ordered spins. Lacking a well-defined moment themselves, the surfboards will possess strong transverse spin fluctuations that we have shown, using a mean-field formalism, can lead to spin-glass freezing in only one direction. This is the first experimental example of a purely magnetic analog of the van der Waals interaction, but such an interaction might be relevant in other systems of nanoscale magnets such as possible *anti*-ferro fluids and artificial spin ice [26]. Furthermore, the well-known connection between the van der Waals force and the Casimir effect [27], in conjunction with the AF version of the former as discussed here, suggests a possible attractive force between plates of AF-ordered spins lying in the plane of the plate. Experiments to measure this force may be possible using microelectromechanical systems.

The data that support the findings of this study are available from the corresponding author upon reasonable request [28].

We acknowledge useful discussions with A. P. Young, W. P. Wolf, D. Huse, and G. Aeppli. This work was supported by the U.S. Department of Energy (DOE) Grants No. DE-SC0017862 (P.G.L and A.P.R.) and No. DE-SC0008832 (T.B. and T.S.). Work by Y.X., T.B. and T.S. was carried out in part at the National High Magnetic Field Laboratory, which is funded by the National Science Foundation under Grant No. NSF-1644779 and the State of Florida. Work at Argonne (S.R. and D.P., neutron scattering and high-temperature susceptibility measurements) was supported by the U.S. Department of Energy (DOE), Office of Basic Energy Science, Materials Science and Engineering Division. Use of the Spallation Neutron Source at ORNL was sponsored by the Scientific User Facilities Division, Office of Basic Energy Sciences, U.S. DOE. Crystal orientation was performed by J. Neu at Florida State University and the National High Magnetic Field Laboratory.

P.G.L. and A.P.R. performed data analysis, drafted the manuscript, and carried out the susceptibility and nonlinear susceptibility measurements. D.P., F.Y., and S.R. performed the neutron-diffraction measurements and analysis. Y.X. performed the EELS measurements shown in the Supplemental Material. T.B. and T.S. performed structural determinations. S.V.S. carried out the theoretical calculations.

The authors declare no competing financial or nonfinancial interests.

[1] A. Abragam and B. Bleaney, *Electron Paramagnetic Resonance of Transition Ions* (Clarendon Press, Oxford, 1970).

[2] W. Wolf, Anisotropic interactions between magnetic ions, J. Phys., Colloq. **32**, 26 (1971).

[3] L. J. Dejongh and A. R. Miedema, Experiments on simple magnetic model systems, Adv. Phys. **23**, 1 (1974).

[4] K. Binder and A. P. Young, Spin-glasses - experimental facts, theoretical concepts, and open questions, Rev. Mod. Phys. **58**, 801 (1986).

[5] P. W. Anderson, Concept of frustration in spin-glasses, J. Less-Common Met. **62**, 291 (1978).

[6] U. Atzmony, E. Gurewitz, M. Melamud, H. Pinto, H. Shaked, G. Gorodetsky, E. Hermon, R. M. Hornreich, S. Shtrikman, and B. Wanklyn, Anisotropic Spin-Glass Behavior in Fe2TiO5, Phys. Rev. Lett. **43**, 782 (1979).

[7] Y. Yeshurun, I. Felner, and B. Wanklyn, Effect of Crystal-Field Anisotropy on Irreversible Phenomena in Spin-Glasses, Phys. Rev. Lett. **53**, 620 (1984).

[8] Y. Yeshurun and H. Sompolinsky, Transverse ordering in anisotropic spin-glasses, Phys. Rev. B **31**, 3191 (1985).

[9] J. K. Srivastava, W. Treutmann, and E. Untersteller, Anisotropic spin glass pseudobrookite: Evidence for transverse freezing and possible implications, Phys. Rev. B **68**, 144404 (2003).

[10] J. Rodrigues, W. S. Rosa, M. M. Ferrer, T. R. Cunha, M. J. M. Zapata, J. R. Sambrano, J. L. Martinez, P. S. Pizani, J. A. Alonso, A. C. Hernandes, and R. V. Goncalves, Spin-phonon coupling in uniaxial anisotropic spin-glass based on Fe_2TiO_5 pseudobrookite, J. Alloys Compd. **799**, 563 (2019).

[11] Y. Yeshurun, J. L. Tholence, J. K. Kjems, and B. Wanklyn, Spin dynamics in the anisotropic spin-glass Fe_2TiO_5, J. Phys. C: Solid State Phys. **18**, L483 (1985).

[12] R. L. Lichti, S. Kumar, and C. Boekema, Spin-glass dynamics In $Fe_{2-X}Ti_{1+X}O_5$, J. Appl. Phys. **63**, 4351 (1988).

[13] The crystals used for this study were obtained from the Bell Labs Crystal Archive, the contents of which can be found at the NSF sponsored website: http://www.crystalsamplearchive.org/, where further details may be found. The particular crystals used in this study were characterized using x-ray diffraction, and electron energy-loss spectroscopy, details of which are found in the Supplemental Material [14].

[14] See Supplemental Material at http://link.aps.org/supplemental/10.1103/PhysRevB.103.L220404 for details of the theoretical calculation as well as information about the EELS sample characterization.

[15] S. Rosenkranz and R. Osborn, Corelli: Efficient single crystal diffraction with elastic discrimination, Pramana-J. Phys. **71**, 705 (2008).

[16] F. Ye, Y. H. Liu, R. Whitfield, R. Osborn, and S. Rosenkranz, Implementation of cross correlation for energy discrimination on the time-of-flight spectrometer CORELLI, J. Appl. Crystallogr. **51**, 315 (2018).

[17] O. Arnold, J. C. Bilheux, J. M. Borreguero, A. Buts, S. I. Campbell, L. Chapon, M. Doucet, N. Draper, R. F. Leal, M. A. Gigg, V. E. Lynch, A. Markvardsen, D. J. Mikkelson, R. L. Mikkelson, R. Miller, K. Palmen, P. Parker, G. Passos, T. G. Perring, P. F. Peterson, S. Ren, M. A. Reuter, A. T. Savici, J. W. Taylor, R. J. Taylor, R. Tolchenoy, W. Zhou, and J. Zikoysky, Mantid-Data analysis and visualization package for neutron scattering and mu SR experiments, Nucl. Instrum. Methods Phys. Res., Sect. A **764**, 156 (2014).

[18] T. M. Michels-Clark, A. T. Savici, V. E. Lynch, X. P. Wang, and C. M. Hoffmann, Expanding Lorentz and spectrum

corrections to large volumes of reciprocal space for single-crystal time-of-flight neutron diffraction, J. Appl. Crystallogr. **49**, 497 (2016).

[19] S. W. Lovesey, *Theory of Neutron Scattering from Condensed Matter Vol II* (Oxford University Press, Oxford, 1984).

[20] H. E. Stanley, *Introduction to Phase Transitions and Critical Phenomena* (Oxford University Press, New York, 1971).

[21] P. Nordblad, L. Lundgren, E. Figueroa, U. Gafvert, and O. Beckman, Critical behavior of the magnetic-susceptibility of Mnf2 near the Néel point, Phys. Scr. **20**, 105 (1979).

[22] V. S. Dotsenko, Physics of a spin-glass state, Usp. Fiz. Nauk. **163**, 1 (1993).

[23] M. Mezard, G. A. Parisi, and M. Virasoro, *Spin Glass Theory and Beyond* (World Scientific, Singapore, 1986), Vol. 9, World Scientific Lecture Notes in Physics.

[24] M. Hasenbusch, A. Pelissetto, and E. Vicari, The critical behavior of 3D Ising spin glass models: Universality and scaling corrections, J. Stat. Mech. (2008) L02001.

[25] H. G. Katzgraber, M. Korner, and A. P. Young, Universality in three-dimensional Ising spin glasses: A Monte Carlo study, Phys. Rev. B **73**, 224432 (2006).

[26] R. F. Wang, C. Nisoli, R. S. Freitas, J. Li, W. McConville, B. J. Cooley, M. S. Lund, N. Samarth, C. Leighton, V. H. Crespi, and P. Schiffer, Artificial 'spin ice' in a geometrically frustrated lattice of nanoscale ferromagnetic islands, Nature (London) **439**, 303 (2006).

[27] M. Bordag, U. Mohideen, and V. M. Mostepanenko, New developments in the Casimir effect, Phys. Rep.: Rev. Sect. Phys. Lett. **353**, 1 (2001).

[28] The data that support the findings of this study are available from the corresponding author upon reasonable request.

Correction: The surname of the fifth author contained an error and has been fixed.

Second Correction: The omission of an acknowledgment statement has been fixed.